Predator-scale spatial analysis of intra-patch prey distribution reveals the energetic drivers of rorqual whale super-group formation

David E. Cade[1,2,*], S. Mduduzi Seakamela[3], Ken P. Findlay[4,5], Julie Fukunaga[1], Shirel R. Kahane-Rapport[1], Joseph D. Warren[6], John Calambokidis[7], James A. Fahlbusch[1,7], Ari S. Friedlaender[2], Elliott L. Hazen[8], Deon Kotze[3], Steven McCue[3], Michael Meÿer[3], William K. Oestreich[1], Machiel G. Oudejans[9], Christopher Wilke[10], Jeremy Goldbogen[1]

* author to whom correspondence should be addressed: davecade@stanford.edu

[1] Hopkins Marine Station, Stanford University, 120 Ocean View Blvd, Pacific Grove, CA 93950, USA

[2] Institute of Marine Science, University of California, Santa Cruz, 115 McAllister Way, Santa Cruz, CA 95060, USA

[3] Department of Environment, Forestry and Fisheries, Branch: Oceans and Coasts, Victoria & Alfred Waterfront, Cape Town, South Africa

[4] Oceans Economy, Cape Peninsula University of Technology, Cape Town, South Africa

[5] MRI Whale Unit, Department of Zoology and Entomology, University of Pretoria, Hatfield, South Africa

[6] School of Marine and Atmospheric Sciences, Stony Brook University, 239 Montauk Highway, Southampton, NY 11968, USA

[7] Cascadia Research Collective, Olympia, WA, USA

[8] Environmental Research Division/Southwest Fisheries Science Center/National Marine Fisheries Service/National Oceanic and Atmospheric Administration, Monterey, CA 93940, USA.

[9] Kelp Marine Research, 1624 CJ Hoorn, The Netherlands

[10] Department of Environment, Forestry and Fisheries, Branch: Fisheries Management, Foretrust Building, Foreshore, Rogge Bay, Cape Town, South Africa

Acknowledgements: We gratefully thank Duke Marine Robotics and Remote Sensing for UAV images, Tamara Goldbogen for data transfer, John Ryan for contributions related to the spatial locations of super-groups, and the crews of the RV FRS Ellen Khuzwayo and the Moss Landing Marine Labs based RV John Martin. All cetacean data collected under NMFS permits 16111, 20430 and South African permits RES2015/DEA and RES2016/DEA. All procedures were conducted under institutional IACUC protocols. This work funded with NSF IOS grant #1656691, ONR YIP grant #N000141612477, Stanford University's Terman and Bass Fellowships, and funding from the South African Department of the Environment, Forestry and Fisheries. Monterey bathymetric data provided by MBARI and NOAA's National Centers for Environmental Information. South African bathymetric data provided by the South African Navy Hydrographic Office.

Author contributions: DEC, SMS, KPF, JC, ASF, ELH, & JAG drove investigation. JDW calculated TS of *E. lucens* and *T. spinifera*. DEC, JF & JAG prepared hydroacoustic data for processing. DEC & SRKR analyzed feeding rates from tag data. DEC, SMS, KPF, DK, SM, MM, MGO, CW, JC, ASF, JAF, ELH, SRKR, WKO & JAG collected field data. DEC processed the hydroacoustic and tag data, performed statistical analyses and led the writing of the manuscript. All authors contributed substantially to revisions and gave final approval for publication.

Data accessibility: Prey and tag data have been deposited at Stanford University's digital repository: https://purl.stanford.edu/rq794kc6747. Monterey bathymetric data used for Fig. 7 is available publically: https://www.ncei.noaa.gov/metadata/geoportal/rest/metadata/item/gov.noaa.ngdc.mgg.dem:3544/html.

Abstract

1. Animals are distributed relative to the resources they rely upon, often scaling in abundance relative to available resources. Yet, in heterogeneously distributed environments, describing resource availability at relevant spatial scales remains a challenge in ecology, inhibiting understanding of predator distribution and foraging decisions.
2. We investigated the foraging behavior of two species of rorqual whales within spatially limited and numerically extraordinary super aggregations in two oceans. We additionally described the lognormal distribution of prey data at species-specific spatial scales that matched the predator's unique lunge-feeding strategy.
3. Here we show that both humpback whales off South Africa's west coast and blue whales off the US west coast perform more lunges per unit time within these aggregations than when foraging individually, and that the biomass within gulp-sized parcels was on average higher and more tightly distributed within super-group associated prey patches, facilitating greater energy intake per feeding event as well as increased feeding rates.
4. Prey analysis at predator-specific spatial scales revealed a stronger association of super-groups with patches containing relatively high geometric mean biomass and low geometric standard deviations than with arithmetic mean biomass, suggesting that the foraging decisions of rorqual whales may be more influenced by the distribution of high-biomass portions of a patch than total biomass. The hierarchical distribution of prey in spatially-restricted, temporally-transient, super-group associated patches demonstrated high biomass and less variable distributions that facilitated what are likely near-minimum intervals between feeding events.
5. Combining increased biomass with increased foraging rates implied that overall intake rates of whales foraging within super-groups were approximately double those of whales foraging in other environments. Locating large, high-quality prey patches via the detection of aggregation hot-spots may be an important aspect of rorqual whale foraging, one that may have been

suppressed when population sizes were anthropogenically reduced in the 20th century to critical lows.

Key words: patchiness, krill, gulp-sized cell, lognormal prey distribution, blue whales and humpback whales, social foraging, filter-feeding, fisheries acoustics, foraging ecology, whale scale

Introduction

Both the density of foraging predators and the types of collective behaviors displayed by groups are strongly driven across taxa by the heterogeneity, or patchiness, of resources in the environment (Piatt & Methven 1992; Gordon 2014), but effectively describing the availability of patchy resources to foragers is a fundamental challenge in ecology (Levin 1992; Benoit-Bird *et al.* 2013; Chave 2013). Baleen whale (Mysticeti) systems are an ideal lens through which to study the physiological drivers and ecological limits related to patchiness because, as capital-breeding bulk filter-feeders, they require dense concentrations of seasonally available prey; essentially, their life history is driven by both spatial (Piatt & Methven 1992; Hazen *et al.* 2009; Hazen, Friedlaender & Goldbogen 2015; van der Hoop *et al.* 2019) and temporal patchiness (Fossette *et al.* 2017; Abrahms *et al.* 2019). Additionally, unusually in pelagic systems it is possible to study both the behavior of baleen whales and the distribution of their euphausiid (krill) prey quantitatively and simultaneously *in situ* via the use of bio-logging tags and hydroacoustic echosounders (e.g. Baumgartner & Mate 2003; Owen *et al.* 2017; Goldbogen *et al.* 2019; Guilpin *et al.* 2019).

Baleen whales are the largest predators of all time, and rorqual whales (in the clade Balaenopteroidea) including blue (*Balaenoptera musculus*) and humpback whales (*Megaptera novaeangliae*), can engulf volumes of water (means ~ 130 and 15 m^3, respectively) that approach or exceed their own body masses (Goldbogen *et al.* 2012; Kahane-Rapport & Goldbogen 2018). Most typically, lunge filter-feeding whales forage singly or in small groups (≤ 3 animals), and large groups of up to 10-20 animals, often fish-feeding humpback whales, have also been reported in some ecosystems (Jurasz & Jurasz 1979;

Whitehead 1983; Kirchner *et al.* 2018). Group membership can be defined spatially or behaviorally according to the process under study (Mann 2000); here we refer to groups as spatially cohesive aggregations, regardless of social, temporal or behavioral affiliations, such that individuals must interact with each other (constructively or destructively) when accessing prey. Topographical or transient oceanographic features (i.e. bays, fronts and upwelling regions) are sometimes associated with very large numbers (200+) of animals distributed over large (10-70 km) spatial extents that can generally be considered to be foraging independently of each other (e.g. Jaquet 1996; Nowacek *et al.* 2011). In contrast, our study involves dense aggregations such that individuals could be in direct conflict for the same resource.

The formation of spatially constricted, large aggregations of humpback whales in close proximity (numbering upwards of 100 whales within five body lengths) have been observed since 2011 in the Benguela Current upwelling region off the west coast of South Africa in a region where previous studies reported only loose aggregations up to 20 animals (Findlay *et al.* 2017). Known as super-groups, similarly large aggregations have been reported historically (e.g. Bruce 1915) and the contemporary reemergence of this behavior may be related to the recovery of regional large whale populations above critical thresholds. Findlay *et al.* (2017) relate that animals in these super-groups are likely foraging, however, group behavior does not necessarily imply optimal behavior (Przybylski *et al.* 2013), and the proximate causes that inspire such large aggregations have not before been explained.

In this study, we examined the prey conditions near, and the foraging behavior of, large aggregations of rorqual whales in two environments: humpback whales in South Africa and blue whales in Monterey Bay off the US west coast (Fig. 1). We hypothesized that the whales observed in super-groups were foraging throughout the environment in which they were observed, but that foraging conditions were of higher quality proximal to super-group observations, suggesting that prey availability is an underlying driver of super-group aggregation. To test this hypothesis, we characterized the prey fields in both environments proximal to foraging whales that were both loosely and densely aggregated by analyzing fisheries acoustics data at spatial scales that match the foraging style of the predators. We show how this method can be used to reveal differences between heavily-foraged patches proximal to large predator

aggregations and other patches in the environment that also appear to contain abundant biomass. We additionally used bio-logging tags in both environments to test whether whales in super-groups demonstrated higher feeding rates than whales not aggregated in super-groups. Illuminating the differences in prey conditions between aggregated and non-aggregated whales may not only explain why super-groups form, but may aid understanding about how predators foraging in a patchy environment make decisions about where and when to expend foraging effort.

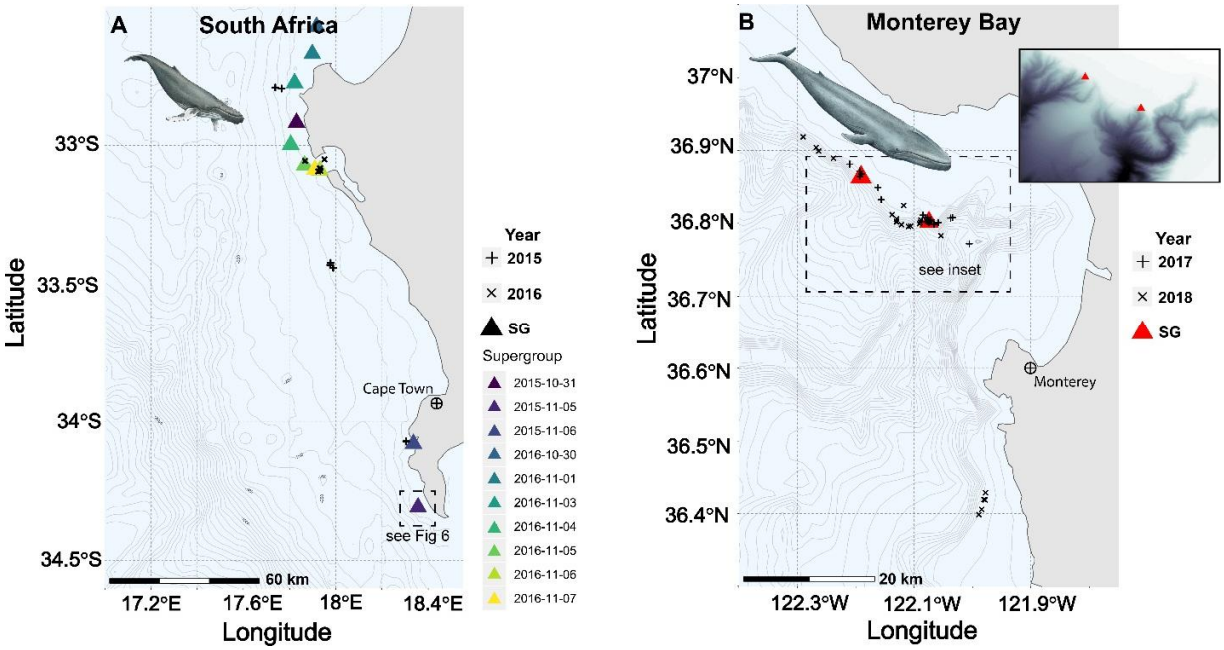

Fig. 1- Field locations in South Africa (A) and Monterey Bay (B). Depth contour lines are separated by 50 m until the 500 m isobath and then 100 m thereafter. Triangles show observed super-group (SG) locations, and + and × mark the deployment locations of suction-attached bio-loggers on humpback (A) and blue whales (B). Data collected near each super-group is collated in Table S1.

Materials and Methods-

We investigated aggregations of rorqual whales in two eastern boundary-current upwelling ecosystems: humpback whales in the Benguela Current off South Africa's west coast in 2015 and 2016 and blue whales in Monterey Bay off the US west coast in 2017 and 2018 (Fig. 1). These aggregations are distinct from other contemporary descriptions of large baleen whale groups in the extraordinary density of

animals within a small region of open ocean – in the case of humpback whales including up to 200 individuals within regions as small as 200 m on a side (Findlay *et al.* 2017) – such that animals must interact with each other as they are foraging (Fig. 2, Video S1). While humpback whale super-groups were the specific focus of research efforts in South Africa, large aggregations of blue whales were encountered only twice opportunistically during Monterey Bay field efforts. For detailed field methods, see Appendix S1 in supporting information.

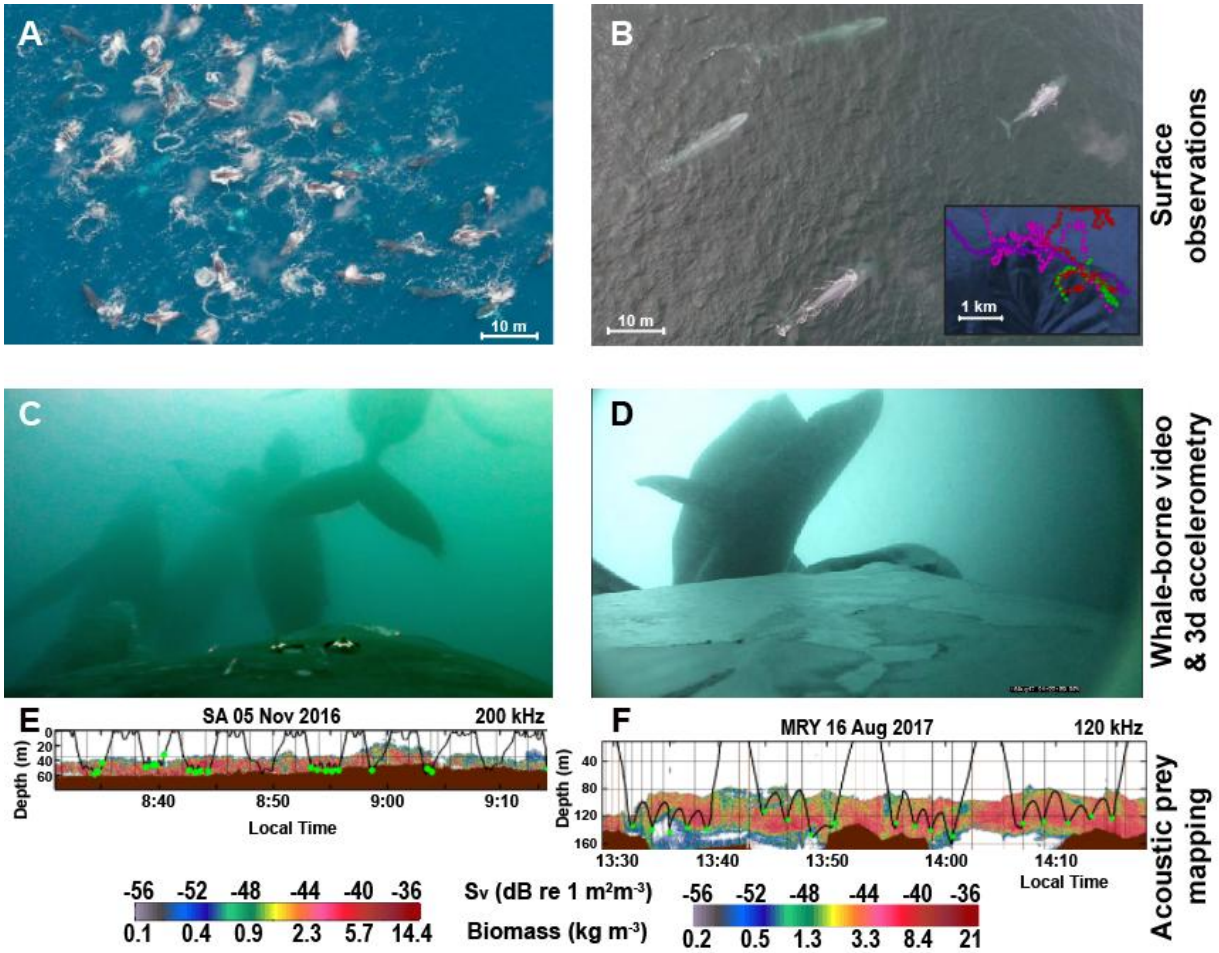

Fig. 2- Investigating super aggregations of predators and prey A) UAV image of at least 60 humpback whales off South Africa's west coast, scale is estimated from mean humpback whale length (image © Jean Tresfon). B) UAV image of four blue whales in an aggregation of ~15 whales in Monterey Bay, CA (image © Duke Marine Robotics and Remote Sensing). Inset: map of super-group region with tracks of tagged whales; the green track represents the topmost whale in the image. C&D) Underwater views of multiple humpback and blue whales, respectively, feeding simultaneously. E&F) Acoustic backscatter near super-group in South Africa and Monterey Bay, respectively, overlaid with the time-synched depth profiles and lunges (green circles) of whales tagged nearby. Grid lines are sized to match the dive-scale unit of analysis for each species.

Foraging behavior

In both locations, to examine foraging behavior within and outside of super-groups we attached integrated 3D accelerometer and video tags to whales for time periods of ~ 2 – 20 hrs. Individual feeding events that involve engulfing a mass of water and krill that can exceed the size of the whale (hereafter, "lunges" or "gulps", see Goldbogen *et al*. 2017) were identified via their kinematic signatures (as in Cade *et al*. 2016). Foraging behaviors including feeding rate (lunges per hour), inter-lunge interval, foraging bout length, and foraging depth were compared within species between super-group and non-super-group times (details in Appendix S1), as well as between the two study ecosystems and among other ecosystems with krill-feeding whales of the same species (total of 112 blue whales and 45 humpback whales, Table 1).

Table 1- Morphometric and feeding parameters that informed analysis, using all krill feeding whales from (Goldbogen *et al.* 2019). Body lengths are representative of whales in the region. Ventral Groove Blubber length (VGB_L) and jaw length (Jaw_L) were allometrically determined (Kahane-Rapport & Goldbogen 2018) and used to create the gulp-size cell (Figs 3&4). Search areas were used to calculate the size of the dive-sized cells. ILI = Inter-lunge interval

Species	Length	VGB_L	Jaw_L	Vertical search area	Horizontal search area	ILI	Lunges per dive	Deployments
B. musculus	22.5 m	12.8 m	4.25 m	44 ± 16 m†	240 ± 119 m†	108 ± 254 s	3.3 ± 2.0	112
M. novaeangliae	10.5 m	6.0 m	2.25 m	35 ± 20 m	125 ± 99 m	43 ± 12 s	3.2 ± 1.1	45

† Search areas for *B. m.* were limited to deployments with georeferenced pseudotracks (n = 51)

To determine the significance of comparisons between super-group and non-super-group foraging of tagged animals, both t-tests and generalized linear mixed effects (GLME) models were used. Foraging of tagged whales when they were and were not in super-groups was compared, and super-group foraging was additionally compared to other whales in the same environment but not in super-groups. Finally, super-group foraging was compared to a larger population of whales outside of the specific tagging period. For humpback whales, this was all krill-feeding whales from CA, the Antarctic and South Africa. For blue whales, this was a comparison with blue whales in the same region as the super-group (Monterey Bay) but a year later. T-tests were used to test for significant differences between mean feeding rates (lunges per hour during foraging bouts) of super-group whales and mean feeding rates of whales foraging when not

aggregated in super groups (Tables 2, S2). For both species, foraging bouts were defined as the time period that included all foraging dives with less than 5.5 minutes (see Appendix S1 and Fig. S4) from the return to the surface of one foraging dive to the start of the next foraging dive. GLME models were constructed in Matlab 2019a for inter-lunge interval (ILI), lunges per dive, dive duration and search area from all data using super-group status as a fixed effect and individual whale as a random effect. For dive duration and lunges per dive, factors known to be influenced by dive depth, mean lunge depth for each dive was binned into 50 m depth bins and used as an additional random effect.

Table 2- Mean feeding parameters derived from tag data for whales foraging in super groups (SG) and not in super groups (NSG). Feeding bout definition described in Fig. S4. Data for individual whales foraging in super-groups (n = 6 in both ecosystems) in Table S2. *M. n. = M. novaeangliae* (humpback whales), *B. m. = B. musculus* (blue whales).

** = p<.05, ** = p<.01, *** = p<.001*

***M. novaeangliae* (South Africa)**	*Feeding rate (lunges per hr within a foraging bout)*		*Inter lunge interval (ILI, s)*		*Inter lunge search area (10^2 m^2)*		*Lunges per dive*	
	SG	NSG	SG	NSG	SG	NSG	SG	NSG
SG animals	55 ± 15	37 ± 18	32 ± 10	40 ± 18	3.4 ± 2.5	8.1 ± 11	4.5 ± 1.5	3.6 ± 2.2
(p-value)	(0.078)		*** (0.000)		*** (0.000)		(0.516)	
number of animals	6	5	6	5	6	3	6	5
All SA *M. n.*	55 ± 15	39 ± 15	32 ± 10	36 ± 16	3.4 ± 2.5	6.6 ± 10	4.5 ± 1.5	4.1 ± 2.5
(p-value)	(0.086)		*** (0.000)		*** (0.000)		(0.492)	
number of animals	6	7	6	7	6	5	6	7
All *M. n.*	55 ± 15	38 ± 16	32 ± 10	44 ± 18	3.4 ± 2.5	11 ± 26	4.5 ± 1.5	4.4 ± 2.1
(p-value)	* (0.028)		*** (0.000)		** (0.006)		(0.913)	
number of animals	6	17	6	33	6	30	6	33
***B. musculus* (Monterey Bay)**	SG	NSG	SG	NSG	SG	NSG	SG	NSG
SG animals	24 ± 2.9	21 ± 5.1	95 ± 17	102 ± 19	36 ± 34	42 ± 40	4.0 ± 0.9	3.3 ± 1.3
(p-value)	(0.214)		(0.187)		(0.083)		(0.387)	
number of animals	6	5	6	5	6	5	6	5
All MRY 2017 *B. m.*	24 ± 2.9	22 ± 3.9	95 ± 17	101 ± 16	36 ± 34	42 ± 32	4.0 ± 0.9	3.3 ± 1.3
(p-value)	(0.200)		(0.126)		* (0.028)		* (0.038)	
number of animals	6	17	6	17	6	17	6	17
SG *B. m.* vs 2018 *B. m.*	24 ± 2.9	18 ± 3.1	95 ± 17	108 ± 22	36 ± 34	57 ± 85	4.0 ± 0.9	4.8 ± 1.4
(p-value)	*** (0.000)		* (0.014)		(0.124)		(0.886)	
number of animals	6	22	6	22	6	22	6	22

Table 3- Definitions of symbols and abbreviations. See Fig. 3 for schematic representation of hierarchical prey distribution calculations. Subscripts *LN* or N before the variable denote lognormal or normal distributions, respectively. See MacLennan, Fernandes and Dalen (2002) for further descriptions of S_v and TS. For further discussion of the calculation of $\hat{B}$ or $\widehat{S_v}$, see Appendix S1 section "Estimating overall intake." See eq. 1 in Appendix S1 for information on calculating *B* from S_v

Symbol	Definition	Units	Scale
⁘	Multiply or divide (the multiplicative correlate to ±)	–	–
B_{gulp}	Biomass density within a gulp-sized cell	kg m^{-3}	Gulp
B_{patch}	Arithmetic mean biomass density within a patch (estimated from Sv_{patch})	kg m^{-3}	Patch
${}_{LN}B_{ws}$	Whale-scale biomass: the distribution of B_{gulp} within a dive-sized cell, estimated from ${}_{N}Sv_{ws}$ and equivalent to geomean(B_{gulp}) ⁘ GSD(B_{gulp})	kg m^{-3}	Dive
$\overline{{}_{LN}B_{ws}}$	Distribution of ${}_{LN}B_{ws}$ within a patch or region, estimated from $\overline{{}_{N}Sv_{ws}}$ and equivalent to geomean(${}_{LN}B_{ws}$) ⁘ GSD(${}_{LN}B_{ws}$)	kg m^{-3}	Patch or region
$\hat{B}$	Estimated arithmetic mean biomass (mean biomass consumed over time) calculated the summary variables geomean(B_{ws}) and GSD(B_{ws}).	kg m^{-3}	Dive, patch or region
geomean	geometric mean	–	–
GSD	Geometric standard deviation	–	–
SD	Standard deviation	–	–
S_v	Mean volume back scatter strength (MVBS)	dB re 1 m^2m^{-3}	–
S_{v_gulp} or Sv_{gulp}	MVBS within a gulp-sized cell	dB re 1 m^2m^{-3}	Gulp
S_{v_patch} or Sv_{patch}	MVBS within a patch	dB re 1 m^2m^{-3}	Patch
S_{v_dive} or Sv_{dive}	MVBS within a dive-sized cell	dB re 1 m^2m^{-3}	Dive
${}_{N}S_{v\_ws}$ or ${}_{N}Sv_{ws}$	Whale-scale Sv: the distribution of Sv_{gulp} within a dive-sized cell, presented as mean(Sv_{gulp}) ± SD(Sv_{gulp})	dB re 1 m^2m^{-3}	Dive
$\overline{{}_{N}S_{v\ ws}}$ or $\overline{{}_{N}Sv_{ws}}$	Distribution of mean(${}_{N}Sv_{ws}$) of all dive-sized cells within a patch or region, presented as mean(${}_{N}Sv_{ws}$) ± SD(${}_{N}Sv_{ws}$)	dB re 1 m^2m^{-3}	Patch or region
$\widehat{S_v}$	Estimated MVBS from a dive, patch or region, calculated from the summary variables mean(S_v) and SD(S_v)	dB re 1 m^2m^{-3}	Dive, patch or region
TS	Target strength (see eq. 1 in Appendix S1)	dB re 1 m^2m^{-3}	–

Prey data collection and initial processing

Prey data were collected using multi-frequency (38 and either 120 or 200 kHz), split-beam fisheries acoustic systems (Simrad EK60s or EK80s) ensonifying the water column below a vessel within an estimated 500 m of foraging whales in both ecosystems, a distance we considered proximal given the size of observed patches. Data collected near super-groups were compared to data collected near feeding whales not aggregated into super-groups on each observation day and in aggregate as described below. Krill

biomass at each analyzed spatial scale was estimated from the mean volume backscattering strength (S_v in dB re 1 m^2m^{-3}, Table 3) of pings aggregated into cells in Echoview v9 with heights and lengths as detailed below. The acoustic set-up, the calculation of target strength for small krill, and the conversion of acoustic units to biomass units are all detailed in Appendix S1. Aggregations of krill, dominated by large swarms > 10 m thick and 1 km across, were identified in Echoview v9 acoustic echograms using the SHAPES school detection algorithm (Barange 1994; Coetzee 2000) and dB differencing techniques (Jarvis *et al.* 2010, additional details in Appendix S1).

Predator-scale prey analysis

Rorqual whales utilize a unique foraging style, lunge filter-feeding, characterized by raptorial targeting of discrete parcels of water followed by filtration through baleen plates and retention of prey (Pivorunas 1979; Goldbogen *et al.* 2017). Typically this behavior consists of diving to depths ranging from the surface to > 300 m, performing one to ten lunges, and then returning to the surface to breathe before diving again. To match the spatial scale of prey analysis to the spatial scale utilized by diving whales, we first used tag data to identify the mean horizontal and vertical distances traveled by foraging whales of both study species from 10 s before the first lunge in a dive to 10 s after the last lunge in a dive (distances in Table 1, details in Appendix S1). We then divided the acoustically identified prey patches (Figs. 3A, 4C-D) into these dive-sized cells (Figs. 3B, 4E-F).

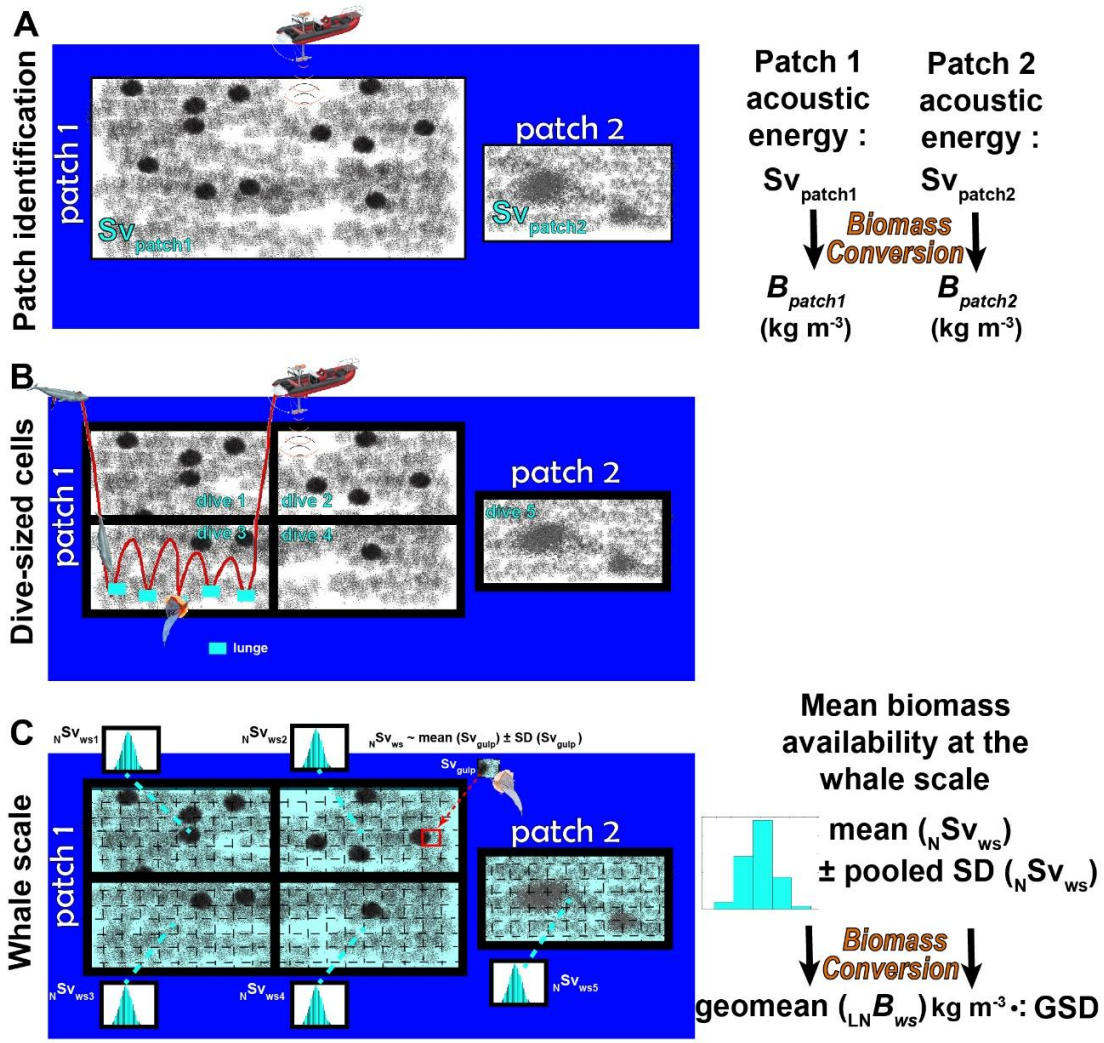

Fig. 3- Schematic illustrating the analytical technique for two acoustically detected prey patches. A) The patch scale is commonly reported in acoustics literature, looking at the linearly averaged mean biomass within each patch. B) In the whale scale approach, patches are first divided into cells the size of an average whale foraging dive (Table 1). C) The whale scale looks at the distribution of the biomass of gulp-sized cells within dives and then pools results for a representation of the mean availability of biomass at the scale experienced by the predator. Biomass conversion equation in Appendix S1, eq. 1. SD = standard deviation, geomean = geometric mean = antilog(mean(log(biomass))), GSD = geometric standard deviation = antilog(SD(log(biomass))). Other symbols defined in Table 3.

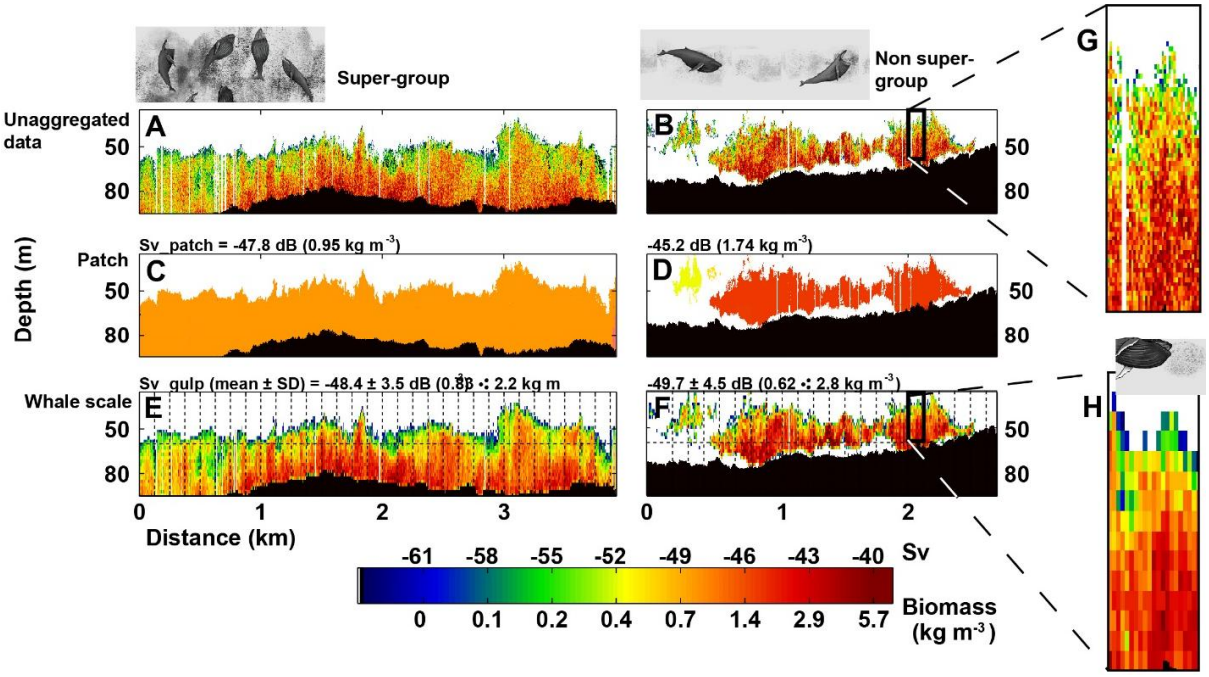

Fig. 4- Matching the spatial scale of rorqual whale feeding with acoustic analysis can illuminate differences between patches that appear to be of similar quality. A&B) hydroacoustic data from super-group and non-super-group regions on 05 Nov 2015, averaged into 1 m x 1 m cells (for display purposes along a consistently sized x-axis). C&D) The mean density of each identified krill swarm as exported from Echoview. The large non-super-group krill swarm in D had nearly double the krill density overall than the swarm in C proximate to a super-group, suggesting that the mean density of krill swarms may not be an appropriate metric to describe prey availability here since at this scale the super-group patch would appear to be lower quality. E&F) The whale scale: the patch is divided into cells the average size of a (2D) humpback whale foraging dive (125 m x 35 m) and then further divided into gulp-sized cells. The geometric mean of the gulp-sized cells within dive-sized cells is higher in the super-group proximal patch. G) acoustic data in a dive-sized cell at fine resolution. H) acoustic data in a dive-sized cell averaged into gulp-sized cells, demonstrating how at this resolution the distribution of krill within the patch is preserved.

To examine the distribution of krill within dive-sized cells (Fig. 3C, 4H), we used Echoview to calculate S_v within analytical cells the size of an average whale engulfment volume (S_{v_gulp}, symbol definitions in Table 3) as calculated from the morphology of an intermediately-sized representative of each species of interest (blue whale total length = 22.5 m, humpback whale = 10.5 m). Jaw length was used for the vertical size of the cell (blue whale = 4.3 m, humpback whale = 2.3 m) and the ventral groove blubber length (blue whale = 12.8 m, humpback whale = 6.0 m) was used for the horizontal cell size (lengths calculated from ordinary least squares regression relationships in Kahane-Rapport & Goldbogen 2018). At the observed prey patch depths, all return echoes had y-axis values larger than the head width, so the extracted cells represented a 2D projection of the gulp size. The engulfed water volume of rorqual whales

is a good spatial match for the analysis of acoustic data since the large size of engulfed water parcels allows multiple acoustic returns to be processed even at our smallest desired spatial scale. Gulp-sized cells contained a minimum of two pings, and in Monterey, blue whale gulp-sized cells averaged 9.4 ± 12.5 pings (mean ± SD), while in South Africa humpback whale gulp-sized cells averaged 8.4 ± 6.8 pings (details in Appendix S1). The variation in the number of pings per gulp is a product of variable speeds by the survey vessel and variable ping rates set to maximize the number of samples without introducing acoustic artefacts like false bottoms. When such variation is present in a survey, data that is averaged into patches without first accounting for survey distance can potentially be biased. We report whole patch S_v (e.g. Fig. 4C,D, Table S3) for comparison to the spatially averaged approach described above.

Characterizing patchy prey

In both marine (Bennett & Denman 1985; Campbell 1995) and terrestrial (White 1978) environments, both inter- (Preston 1948; Preston 1962; Pagel, Harvey & Godfray 1991; Magurran & Henderson 2003) and intra- (Barnes 1952; Anand & Li 2001) species abundances tend to be distributed heterogeneously and can often be characterized by lognormal distributions (Dennis & Patil 1987). That is, the log of abundance data is typically normally distributed and can be characterized by the mean and standard deviation of logged data, or, equivalently, the geometric mean and geometric standard deviation of the unlogged data. Fisheries acoustics data, however, are typically reported as overall mean abundance integrated over broad areas (e.g. Croll *et al.* 1998; Benson *et al.* 2002; Cox *et al.* 2009; Nickels, Sala & Ohman 2019) or mean volumetric density within patches (e.g. Nowacek *et al.* 2011; Hazen, Friedlaender & Goldbogen 2015; Owen *et al.* 2017). Prey patches can be heterogeneously distributed in space (Watkins & Murray 1998; Kaartvedt *et al.* 2005; Benoit-Bird, Waluk & Ryan 2019), however, and aggregations themselves can have variable structure (Benoit-Bird, Moline & Southall 2017), implying that using a single number to characterize the biomass density of a large patch may not represent what a foraging animal encounters (Stephens & Krebs 1986). Additionally, averaging the biomass densities among patches with

variable sizes may misrepresent mean availability if biomass is not weighted by patch size, or if acoustic surveys with variable ping rates or vessel speeds are not first averaged into spatially consistent regions.

When prey patches are small such that a lunge-feeding whale feeds on it only once, describing patch density with a single number for each krill patch would be an appropriate strategy. However, the krill swarms we observed in this study were several km across (Fig. 2) such that predators could be considered to be foraging within a patch rather than among patches. Consequently, to better represent the prey biomass available to foraging rorqual whales, we characterized the prey fields proximal to feeding whales at predator-specific spatial scales, dividing large patches into analytical cells the size of an individual whale's gulp and then examining how those gulp-sized cells are distributed within cells of a size likely experienced by whales on a foraging dive (Figs. 3-4). These gulp-sized cells are distributed, as in patchy prey in other aquatic and terrestrial systems, lognormally (more details in Appendix S1, Fig. S1). Details for estimating mean intake from lognormal distributions are also reported in the Appendix S1 section "Estimating overall intake."

The whale scale

For each dive-sized cell in a region of interest (e.g. all dive sized-cells proximal to a super-group on a specific day), we first summarized the distribution of biomasses likely to be experienced by a foraging whale on a dive by calculating the mean and standard deviation (SD) of S_{v_gulp} within each dive-sized cell. To ensure sufficient statistical power, only cells that had at least thirty gulp-sized cells were included in analysis. We then summarized the overall distribution in super-group associated patches and patches not associated with super-groups by averaging all dive summary values ($_{N}S_{v\_ws}$) in a region and calculating the pooled SD of all dives within the region of interest (Fig. 3C). We refer to this summarized analysis of prey as the mean "whale scale" ($\overline{}_{N}S_{v\_ws}$ in acoustic units, $\overline{}_{LN}B_{ws}$ in estimated biomass units, Table 3).

All statistical comparisons were done on the acoustic units which have approximately normal distributions, and then S_v was converted to estimated biomass (generally following Jarvis *et al.* 2010, with

study system specific calculation details in Appendix S1). Because biomass estimation is subject to model enhancements over time, we report S_v (as mean ± pooled SD) throughout the text in addition to biomass (*B*, Table 3). Biomass of gulp-sized cells (B_{gulp}) was lognormally distributed at larger scales (Fig. S1), so for whale-scale summary values we present the geometric mean (geomean) and the geometric standard deviation (GSD) of gulp-sized cells (B_{gulp}). The geomean and GSD are equivalent to the antilog of the mean and SD of log(biomass). There are several advantages to summarizing data using lognormal distributions instead of reporting mean biomass including less sensitivity to outliers and a better ability to characterize the spread of data. We report lognormal summary statistics as "biomass in kg m^{-3} •⁚ a multiplicative scalar", where •⁚ is read "multiplied or divided by" and is a combination of the multiplication (•) and division (⁚) symbols introduced by Leibniz (1684). •⁚ can be interpreted as the multiplicative complement to the commonly used ±.

The whale scale analytical scale – the distribution of gulp-sized cells within its corresponding dive-sized cell (Fig. 3C, Fig. 4E,F) – can be thought of as the spread of biomass around a dive's median biomass. We developed this scale because of its link to the spatial scale of prey experienced by foraging rorqual whales on any given foraging dive. This analytical technique gives a representation of what a foraging rorqual could encounter on a dive and would represent what it is likely to forage on if it forages indiscriminately during its dive. However, to account for the likelihood that rorquals employ an active selection strategy to maximize their prey intake we additionally analyzed the distribution of only the top 50% of gulp-sized cells within dive-sized cells. The choice of 50% as a threshold was selected as a compromise between indiscriminate feeding centered around a patch's median and precise selection of gulps with maximum density given how much is unknown about the behavioral patch selection algorithm employed by rorqual whales. We refer to this technique as the "informed whale-scale" analysis and it can be thought of as the distribution of biomass around the 75^{th} percentile of biomass in a dive-sized cell.

Results

Humpback whale super-groups off South Africa's west coast are described in detail in Findlay *et al.* (2017) and consist of 20-200 whales surfacing haphazardly in an area as restricted as 200 m on a side (Fig. 2A, Video S1). Super-groups were observed on 10 of 20 ship days in 2015-2016 (Fig. 1). The duration of super-group cohesiveness is unknown as none were observed from formation to dispersal, but all were observed for at least one hour and in all five instances where group dispersion was observed, emigration was sequential. Unlike in other environments where humpback whales have been observed coordinating their fish-feeding behavior (Jurasz & Jurasz 1979; Wiley *et al.* 2011; Mastick 2016), underwater video evidence suggests that lunge-feeding within these krill patches is uncoordinated (e.g. Video S1). Two blue whale super-groups were encountered in four field days in 2017 in Monterey Bay, California, USA and consisted of an estimated 15-40 whales surfacing within sight of an observer at sea level (~ 1 km range); no super-groups were encountered in nine field days in 2018. Blue whales generally forage in singles or in pairs and the super-groups we observed consisted of many singles and pairs feeding in the same area in an apparently uncoordinated fashion. Due to the similarities in behavior and the much larger sizes of blue whales (blue whales are ~ 2x the length, 4x the mass and have 8x the engulfment capacity of humpback whales, Kahane-Rapport & Goldbogen 2018) we propose that the observed group sizes are comparable despite their differences in individual predator abundances. The blue whale super-group encountered on Aug 14 (25-40 whales estimated) was encountered at 08:30 and had begun to decrease in density at ~11:15. On Aug 16 the group (15-20 whales estimated) was encountered at 13:30 and our vessels left the area at 14:20.

Foraging behavior

All whales fed continuously (accounting for surface recovery and transit time) while in super-groups. Humpback whales fed at a mean depth of 43 ± 13 m while blue whales fed at 109 ± 30 m (e.g., Fig. 2). In both cases, whales in super-groups had similar lunges per dive as non-super-group whales (Table 2),

but the smaller ILI and area traversed between lunges for whales in super-groups compared to non-super-groups (Table 2) led to shorter dive durations (model estimates accounting for foraging depth differences, blue whale 95% confidence interval (CI): 197 to 391 s shorter, humpback whale 95% CI: 60 to 112 s shorter). These factors combined to influence the overall feeding rate, as measured in lunges per hour during feeding bouts, which were 49 and 14% higher, respectively, in humpback whale and blue whale super-groups vs feeding rates when these same whales were not feeding in super-groups, and were 45 and 34% higher, respectively, when super-group whales were compared to krill-feeding whales more generally (Table 2). The increased feeding rates in super-groups suggested that we would find that prey near super-group were distributed in such a way as to facilitate decreased search times.

Prey analysis

Analysis of prey abundance and distribution revealed high-quality foraging conditions in both super-group and non-super-group behavior states in each ecosystem. Identified prey patches near foraging whales were typically 10s of m thick and 100s of m wide, regardless of group size, such that whales could be described as foraging within a patch rather than among patches (Fig. 2, Video S1). Examination of the distribution of the biomass of gulp-sized cells from all identified patches on each survey day revealed the biomass density was distributed lognormally (Fig. S1, Appendix S1), suggesting the appropriateness of the "whale scale" analytical technique for describing the prey field experienced by these large predators. Describing skewed data using the lognormal parameters (geomean and GSD) has the additional advantage of being less sensitive to outliers in the data, and summarizing acoustic data into spatially determined cells has the advantage of matching the spatial scale of collection with the spatial scale experienced by the predator of interest.

In comparing the prey fields in super-group and non-super-group regions, we found that prey density was generally higher in super-group than in non-super-group regions. On ten of eleven observation days (Table S3, Fig. 5) geomean prey density at the whale scale ($\overline{{}_{LN}B_{ws}}$) was higher near super-groups than

near foraging whales not in super-groups ($p < 0.001$ in both environments): blue whale gulps in super-groups averaged 1.5 •: 1.6 kg m^{-3} (-47.5 ± 2.2 dB) while gulps in non-super-groups averaged 1.2 •: 1.8 kg m^{-3} (-48.5 ± 2.6 dB), and humpback whale gulps in super-groups averaged 0.49 •: 2.0 kg m^{-3} (-50.7 ± 3.0 dB) while non-super-group gulps averaged 0.31 •: 2.1 kg m^{-3} (-52.7 ± 3.3 dB). In three of eleven days, prey density was lower near super-groups if prey was described using whole patch means (further discussed below). Patches were additionally substantially and significantly thicker near super-groups in all cases (mean in South Africa: 22 ± 14 m vs 8 ± 9 m, mean in Monterey: 33 ± 27 m vs 15 ± 15 m, Fig. 5, Table S3).

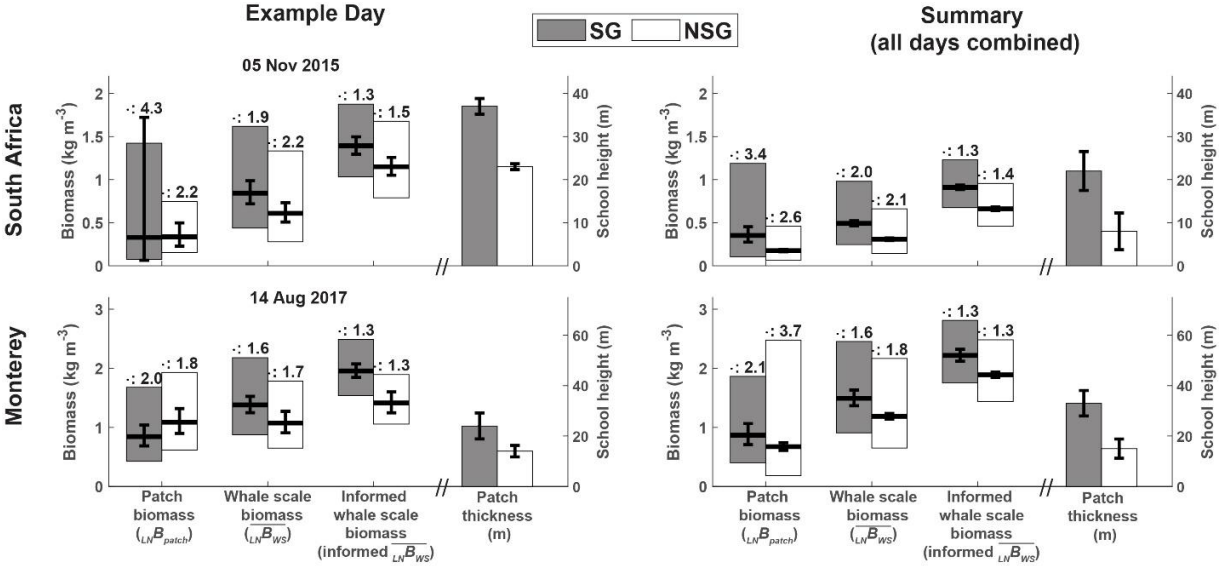

Fig. 5- Summary prey data from an example day and in aggregate for both South Africa and Monterey. Summary data for all days is displayed in Table S3. Symbol definitions in Table 3, SG = super-group, NSG = non-super-group. Prey patch geometric means are the thick horizontal bars, and the large bars represent the GSD with the multiplicative factor listed above each bar. Error bars arround the geometric means are the 95% confidence intervals (calculated in acoustic units and converted to biomass). Patch thickness error bars are 95% confidence intervals.

The GSD of gulps at the mean whale scale was not significantly different between super-groups and non-super-group patches on any given day (Table S3). In 9 of 10 cases the mean gulp at the mean informed whale scale (i.e., the mean gulp within the denser half of dive-sized cells) was significantly higher in super-groups, and in all cases the SD of gulp density at the informed whale scale was 0.1-0.6 dB lower in super-groups than non-super-groups.

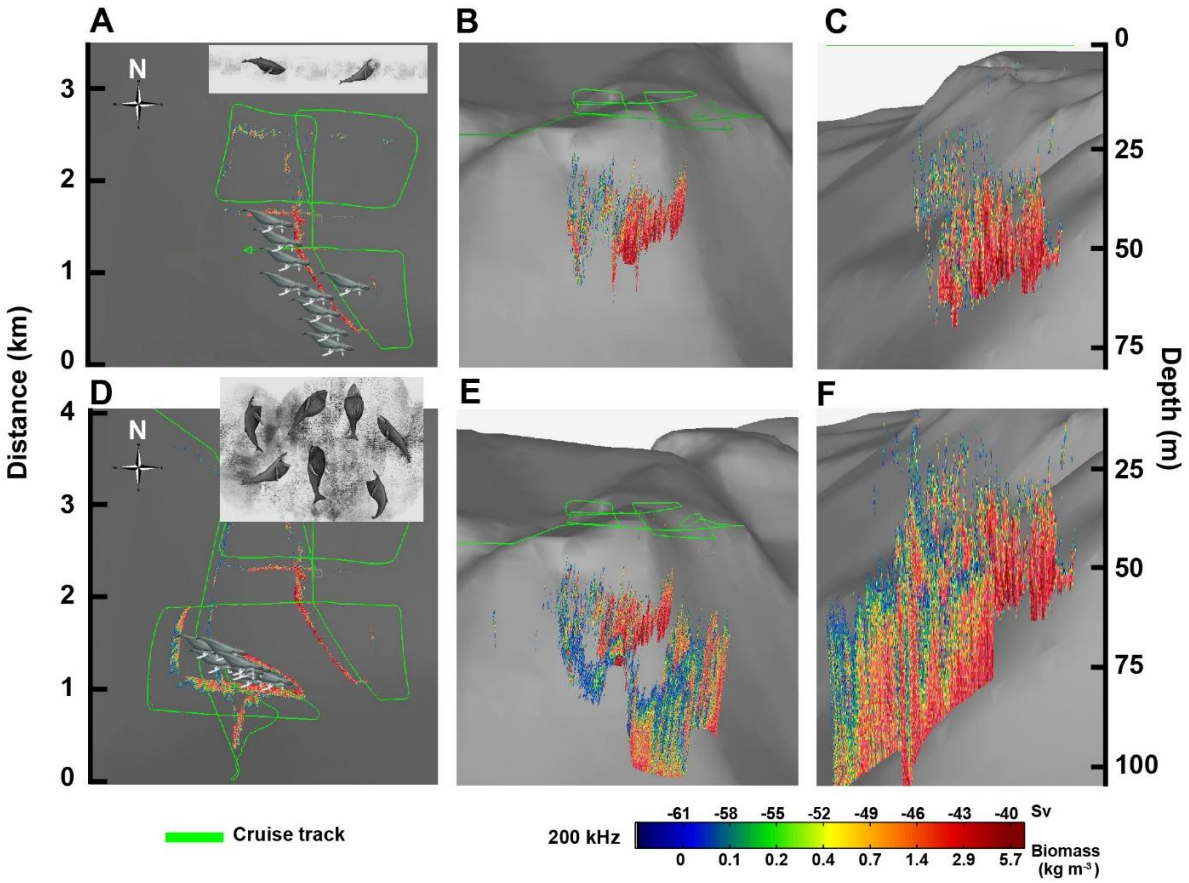

Fig. 6- 3d view of super-group associated prey patch on 05 Nov 2015 in South Africa (the southernmost group in Fig. 1). These are the same data from which Fig. 4 was created. A-C) prey and whales spread out before super-group formation (prey data shown until 17:00 local time). A) overhead view. B) Oblique view (from the northwest), highlighting the prey in relation to submarine canyon bathymetry. C) Side-on view, looking from the south. D-F) Same views now including super-group-associated data when 150-200 whales converged into a region ~ 200 m on a side at ~17:00. Bad weather on this day precluded suction-cup tag deployment. Whale illustrations by Alex Boersma. Bathymetry courtesy of the South Africa Navy Hydrographic Office. Data plotted in Echoview v10 using a 50x vertical exageration.

Prey conditions in the same region both before and during super-group formation were observed just once in South Africa on 05 Nov 2015 (Fig. 4, Fig. 6). In that case, 150-200 whales were spread out along a shelf break before coming together into a single aggregation (Fig. 6). Prey density in patch averages was not significantly different before or during super-group formation ($p > 0.9$, Fig. 5). However, the geomean of gulps at the mean whale scale was 38% higher ($p = 0.010$) in super-group associated patches and was 21% higher at the mean informed whale scale ($p = 0.002$). Additionally, mean patch thickness was

estimated to be 14 m larger in super-groups ($p < 0.001$), and gulp GSD at both the whale scale and the informed whale scale was smaller in super-groups, though only significantly so at the informed whale scale (Fig. 5, Table S3).

In Monterey Bay, the blue whale super-group on 14 Aug 2017 had a similar pattern as the 05 Nov 2015 humpback whale super-group (Fig. 5). While the geomean of patch biomass was smaller (but not significantly different) in the prey field near the observed super-group, geomean gulp biomass at the mean whale scale and the mean informed whale scale were both significantly and substantially higher (Fig. 5, Table S3), and patch thickness and gulp GSD at the informed whale scale were significantly higher and lower, respectively ($p<0.001$ in both cases, Table S3). While the super-group associated patch on 16 Aug 2017 had slightly higher geomean biomass at the whale scale and in patches, results were non-significant (Table S3). Instead, prey around this super-group was characterized by a 2.5-fold increase in patch thickness as well as both a significant increase in geomean gulp biomass density and significant reduction in gulp GSD at the informed whale scale (Table S3).

Patches near super-groups thus had more available biomass on average than patches near whales not in super-groups. In both environments, better quality of super-group patches was indicated by higher geomean gulp density, thicker patches and indications that the prey at the informed whale scale (the denser half of the prey in each dive-sized cell) was more uniform in distribution (i.e. displayed smaller variance).

Discussion

Our results suggest that the formation of super-groups of two species of rorqual whales was largely influenced by high-quality foraging conditions. Gulp-sized cells analyzed at the whale scale had higher geomean biomass and lower variability within prey patches associated with super-groups of humpback and blue whales, and whales within super-groups demonstrated higher feeding rates than more dispersed individuals. Furthermore, characterizing the intra-patch distribution of krill biomass appears to offer an explanation for the higher feeding rates observed in super-groups. Specifically, we found that super-groups

were strongly associated with patches characterized y high geomeans and low GSD of biomass, particularly in the densest half of gulps within dive-sized cells (the informed whale scale). Higher geomeans implies that even a naïvely foraging whale would benefit from increased energy intake at each feeding event, and a lower GSD (when paired with a high geomean) implies that a greater proportion of gulp-sized parcels would be of sufficient quality to feed (i.e., a greater proportion of gulps were above a threshold at which it would be beneficial to feed), enabling the observed increase in lunge feeding events per unit time by decreasing search time. The match of predator behavior (increased feeding rates) with our findings of higher density with less variance in cells the size of what a predator will experience on a foraging dive additionally supports the whale scale level of analysis.

In ecological models of foraging in patchy environments, patch quality is often assessed as the overall intake (per unit time) enabled by an ecosystem (Giraldeau & Caraco 2000). To improve the efficacy of such models, the intake rate parameter, λ, could further be decomposed into two component parts: 1) the energetic quality of each captured prey parcel and 2) the rate at which prey are captured. In rorqual whale foraging systems, these quantities are represented by the mean biomass density in each gulp (λ_ρ) and the lunge rate per unit time (λ_f), respectively, such that $\lambda = \lambda_\rho \times \lambda_f$. We found that prey patches associated with super-groups not only had 40-50% more biomass in the median (geomean) gulp than patches not associated with super-groups, implying higher λ_ρ, but also had smaller GSD. The small GSD implied that prey was of more uniform quality proximal to super-groups, making it easier for whales to maximize consumption without spending time between lunges searching for the best nearby parcel. This reduction in search time likely facilitated the observed increases in super-group λ_f by decreasing the inter-lunge interval as well as the spatial distance traveled between lunges (Table 2). Indeed, the reported super-group feeding rates in both study areas (humpback whales: 55 ± 15 lunges/hr, blue whales: 24 ± 2.9 lunges/hr, Table 2) are comparable to the highest reported rates for whales in other studies: Goldbogen *et al.* (2008) report that one tagged humpback whale fed at a rate of 45 lunges/hr over 8 hrs, Owen *et al.* (2017) report humpback feeding rates of 49 lunges/hr, while Southall *et al.* (2019) report blue whale feeding rates over 10 minute bins that range from 5 to 30 lunges/hr when foraging, with mean rates typically less than 20 lunges/hr and max rates

over foraging bout-comparable time scales of approximately 25 lunges/hr. The high rates of foraging in super-groups suggests that these whales are feeding at rates close to their biomechanical limits.

The analysis of prey at the nested scales we describe is particularly well-suited for describing prey conditions available to krill-feeding rorqual whales because their foraging style utilizes characteristics of both filter-feeding, where energy cost per foraging event is independent of the quality of the prey, and raptorial feeding in which prey (i.e. in bulk patches) are engulfed in discrete units. The combination of these feeding modes distinguishes rorquals from right whales (*Eubalaena glacialis*), whale sharks (*Rhinocodon typus*) and other continuous ram filtration feeders. From our meta-analysis of data from 45 blue whales and 21 humpback whales that lunged multiple times per dive and for which georeferenced tracks could be calculated, we found that those two species traverse an average of 177 ± 51 and 73 ± 34 horizontal meters between lunges and average 4.1 ± 1.4 and 5.2 ± 2.3 lunges per dive, respectively, yet the distance traveled for one lunge is only the length of the buccal cavity (12.8 and 6.0 m, respectively, for a 22.5 m blue whale and 10.5 m humpback whale). Right whales, approximately the same length as humpback whales, are continuous ram filtration filters that filter an average of 670 m^3 of water on every dive (van der Hoop *et al.* 2019). At 14 m^3 of water engulfed per lunge (Kahane-Rapport & Goldbogen 2018), a humpback whale would have to lunge 48 times per dive (an order of magnitude more than their average) to filter an equivalent volume. These factors, combined with the ability to feed on more maneuverable prey enabled by high-speed, raptorial approaches (Cade *et al.* 2020), imply that rorqual whales may be energetically required to make active choices regarding what patch and what part of a patch to feed on, further supporting analysis at the informed whale scale.

Matching the spatial scale of analysis to the scale of the event under study is particularly critical in patchy environments (Levin 1992; Benoit-Bird *et al.* 2013). Although the sensory mechanisms by which rorqual whales determine patch quality in the environment is currently unknown, insights into the process can be gleaned by proposing and examining potential behavioral algorithms used by whales to maximize their energy intake (Hein *et al.* 2020). Prior work has proposed that baleen whales initiate foraging when prey is available above a certain density (Mayo & Marx 1990; Cotté & Simard 2005; Hazen *et al.* 2009;

Feyrer & Duffus 2015; Kirchner *et al*. 2018). Our findings extend these ideas by suggesting that the density and distribution of encountered prey is a better indicator of where whales forage than overall patch or regional abundance. Future work may be able to refine this general principle into a prediction for a behavioral algorithm that would describe under what conditions a whale would give up foraging in one environment to take advantage of an environment it perceives as more favorable.

Better matching the scale of prey distribution to the scale of predator foraging effort could also be used to better predict overall intake rates (λ). Considering that super-groups of two species of whales aggregated in regions with less variability in the densest half of the cell, and given that rorquals are likely not feeding indiscriminately, we suggest that the actual prey consumed by foraging rorqual whales would likely be reflected by the biomass of prey available at the whale scale as a lower bound, but be even better reflected by analysis at the informed whale scale, and we include suggestions for the calculation of these bounds in Appendix S1. Additional studies to quantify a more precise threshold for the informed whale scale could eventually shed light on how rorquals maximize their foraging efficiency in a given environment.

Although humpback and blue whale super-groups have only been recently described, abnormally large densities of krill do not appear to be a new phenomenon. Nicol *et al.* (1987) report surface swarms of *E. lucens* near our study area in South Africa of up to 35 kg m^{-3}. The historical record of super-groups (Bruce 1915) followed by a lack of observed occurrences during periods of low cetacean abundance combined with consistent aggregations of krill suggest that rorqual whale super-groups were once a more common occurrence. Given the 20%-60% increase in geomean prey density we found in super-groups and the concurrent 33-45% increase in feeding rates compared to non-super-group environments, it is likely that super-groups were once an important part of rorqual whale foraging ecology before anthropogenic hunting removed more than three million whales globally (Rocha, Clapham & Ivashchenko 2014). It is plausible, therefore, that recovering populations benefit from a positive feedback loop whereby increased population sizes increase the likelihood of discovering extensive but ephemeral (Fig. 7) patches since concentrations of calling whales, even if calling is not directly related to patch quality or extent, could serve

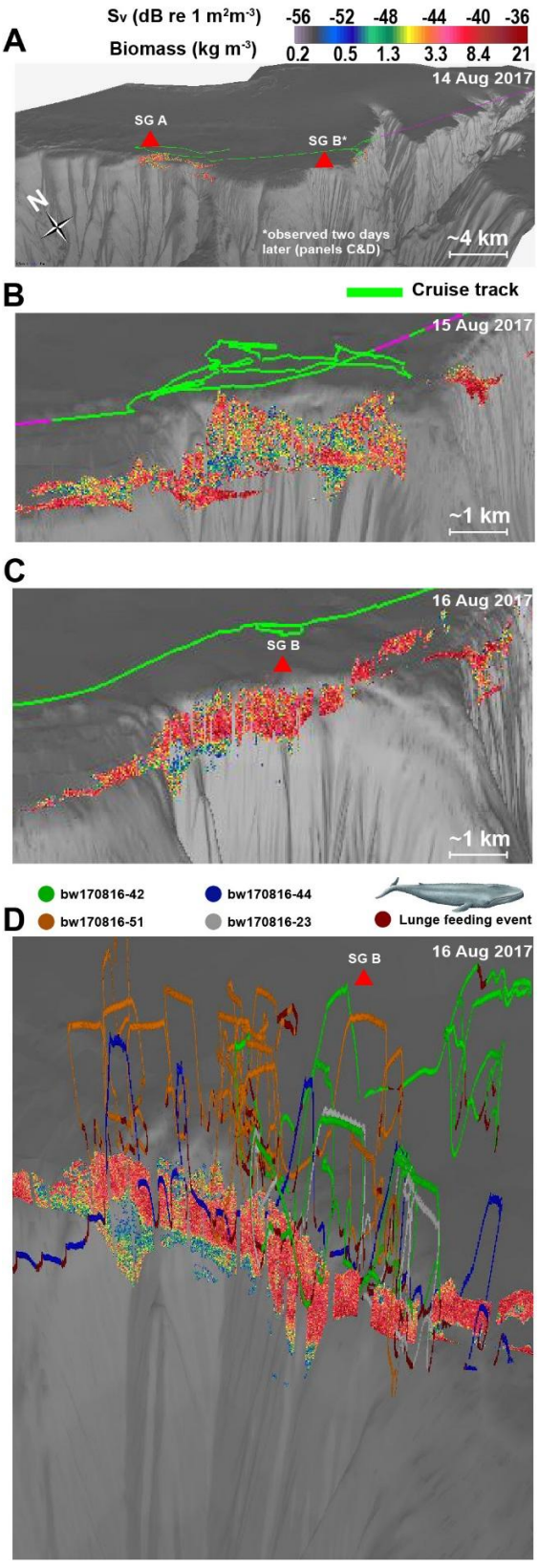
A
Sv (dB re 1 m²m⁻³)
-56 -52 -48 -44 -40 -36
Biomass (kg m⁻³)
0.2 0.5 1.3 3.3 8.4 21
14 Aug 2017
SG A
SG B*
N
*observed two days later (panels C&D)
~4 km
B
Cruise track
15 Aug 2017
~1 km
C
16 Aug 2017
SG B
~1 km
D
bw170816-42
bw170816-44
bw170816-51
bw170816-23
Lunge feeding event
16 Aug 2017
SG B

Fig. 7- 3d view of super-group (SG) associated prey patches in Monterey Bay, CA, USA. A) Overall layout of the north Monterey Canyon edge with prey data near SG A on 14 Aug 2017. B) zoomed in plot of the SG B location, but the day before the SG was noticed. There were scattered blue whales feeding in this area, but it is noticeable how much less uniform and diffuse the high-quality parts of this large patch are. C) zoomed in plot of the SG B associated patch on 16 Aug 2017. D) view from the southeast of the same patch, overlain with tracks from the four tagged whales feeding within SG B. Data plotted in Echoview v10 using a 10x vertical exageration.

as a signpost for wanderers about the location of ephemeral high-quality foraging grounds (Wilson *et al.* 2018). This socially-mediated information exchange would decrease the search time of individuals who might not otherwise find the highest quality regions within a foraging ground (LaScala-Gruenewald *et al.* 2019; Hein & Martin 2020).

The spatial colocation of the observed super-group associated patches with bathymetric features, including small scale (1-5 km wide) canyons that incise typical rorqual foraging habitat regions off the edges of continental shelves (Figs 1, 6, 7), suggest that the two environments in our study may have a specific proclivity to support large, dense prey patches due to the interaction of bathymetry and local oceanographic process that have been shown to aggregate zooplankton (e.g. Santora *et al.* 2018; Benoit-Bird, Waluk & Ryan 2019). Future work examining the spatiotemporal links between mesoscale oceanographic processes, local bathymetry, and temporally transient prey conditions may better help explain how these large predators effectively exploit prey in spatially and temporally complex habitats.

It was not until relatively recently in the fossil record (5-7 Ma) that baleen whales developed gigantic body sizes (> 10 m), and it is likely that this large change came about in concert with oceanic conditions that favored annually consistent upwelling zones that brought nutrient-rich water to the surface in specific areas, creating natural aggregation areas (Slater, Goldbogen & Pyenson 2017). Locating and exploiting these prey hotspots is essential to the foraging strategy of rorqual whales, and we found that differentiating the highest quality prey areas (as characterized by high geometric means and low GSD) from merely good prey areas can result in a doubling of intake rates (λ) when increased feeding rates (λ_f) are combined with increased prey density (λ_ρ). We have described two disparate environments in which predator patchiness – indicated by temporally transient and spatially limited super-group formation – is driven by prey patchiness, and we utilize predator-specific prey density metrics to characterize high-quality

whale habitat. Our results suggest that foregoing local foraging within good prey environments in favor of traversing to great prey environments where conspecifics are aggregating may be an evolutionarily stable strategy when such prey patches are extensive and ephemeral, and future research may reveal the specific social drivers that cue whales into the locations of these high-quality foraging hot spots.

References

Abrahms, B., Hazen, E.L., Aikens, E.O., Savoca, M.S., Goldbogen, J.A., Bograd, S.J., Jacox, M.G., Irvine, L.M., Palacios, D.M. & Mate, B.R. (2019) Memory and resource tracking drive blue whale migrations. *Proceedings of the National Academy of Sciences,* 116, 5582-5587.

Anand, M. & Li, B. (2001) Spatiotemporal dynamics in a transition zone: patchiness, scale, and an emergent property. *Community Ecology,* 2, 161-169.

Barange, M. (1994) Acoustic identification, classification and structure of biological patchiness on the edge of the Agulhas Bank and its relation to frontal features. *South African Journal of marine science,* 14, 333-347.

Barnes, H. (1952) The use of transformations in marine biological statistics. *ICES Journal of Marine Science,* 18, 61-71.

Baumgartner, M.F. & Mate, B.R. (2003) Summertime foraging ecology of North Atlantic right whales. *Marine Ecology Progress Series,* 264, 123-135.

Bennett, A.F. & Denman, K.L. (1985) Phytoplankton patchiness: inferences from particle statistics. *Journal of Marine Research,* 43, 307-335.

Benoit-Bird, K.J., Battaile, B.C., Heppell, S.A., Hoover, B., Irons, D., Jones, N., Kuletz, K.J., Nordstrom, C.A., Paredes, R. & Suryan, R.M. (2013) Prey Patch Patterns Predict Habitat Use by Top Marine Predators with Diverse Foraging Strategies. *Plos One,* 8, e53348.

Benoit-Bird, K.J., Waluk, C.M. & Ryan, J.P. (2019) Forage Species Swarm in Response to Coastal Upwelling. *Geophysical Research Letters,* 46, 1537-1546.

Benoit-Bird, K.J., Moline, M.A. & Southall, B.L. (2017) Prey in oceanic sound scattering layers organize to get a little help from their friends. *Limnology and Oceanography,* 62, 2788-2798.

Benson, S.R., Croll, D.A., Marinovic, B.B., Chavez, F.P. & Harvey, J.T. (2002) Changes in the cetacean assemblage of a coastal upwelling ecosystem during El Niño 1997–98 and La Niña 1999. *Progress in Oceanography,* 54, 279-291.

Bruce, W. (1915) Some observations on Antarctic cetacea. *Scotia Natl. Antarct. Exped. Rep,* 4, 491-505.

Cade, D.E., Carey, N., Domenici, P., Potvin, J. & Goldbogen, J.A. (2020) Predator-informed looming stimulus experiments reveal how large filter feeding whales capture highly maneuverable forage fish. *Proceedings of the National Academy of Sciences,* 117, 472-478.

Cade, D.E., Friedlaender, A.S., Calambokidis, J. & Goldbogen, J.A. (2016) Kinematic Diversity in Rorqual Whale Feeding Mechanisms. *Current Biology,* 26, 2617-2624.

Campbell, J.W. (1995) The lognormal distribution as a model for bio-optical variability in the sea. *Journal of Geophysical Research: Oceans,* 100, 13237-13254.

Chave, J. (2013) The problem of pattern and scale in ecology: what have we learned in 20 years? *Ecology Letters,* 16, 4-16.

Coetzee, J. (2000) Use of a shoal analysis and patch estimation system (SHAPES) to characterise sardine schools. *Aquatic Living Resources,* 13, 1-10.

Cotté, C. & Simard, Y. (2005) Formation of dense krill patches under tidal forcing at whale feeding hot spots in the St. Lawrence Estuary. *Marine Ecology Progress Series,* 288, 199-210.

Cox, M.J., Demer, D.A., Warren, J.D., Cutter, G.R. & Brierley, A.S. (2009) Multibeam echosounder observations reveal interactions between Antarctic krill and air-breathing predators. *Marine Ecology Progress Series,* 378, 199-209.

Croll, D.A., Tershy, B.R., Hewitt, R.P., Demer, D.A., Fiedler, P.C., Smith, S.E., Armstrong, W., Popp, J.M., Kiekhefer, T. & Lopez, V.R. (1998) An integrated approch to the foraging ecology of marine birds and mammals. *Deep Sea Research Part II: Topical Studies in Oceanography,* 45, 1353-1371.

Dennis, B. & Patil, G.P. (1987) Applications in Ecology. *Lognormal distributions* (eds E.L. Crow & K. Shimizu), pp. 303-330. Marcel Dekker New York.

Feyrer, L.J. & Duffus, D.A. (2015) Threshold foraging by gray whales in response to fine scale variations in mysid density. *Marine Mammal Science,* 31, 560-578.

Findlay, K.P., Seakamela, S.M., Meÿer, M.A., Kirkman, S.P., Barendse, J., Cade, D.E., Hurwitz, D., Kennedy, A., Kotze, P.G.H., McCue, S.A., Thornton, M., Vargas-Fonseca, O.A. & Wilke, C.G. (2017) Humpback whale "super-groups" – A novel low-latitude feeding behaviour of Southern Hemisphere humpback whales (*Megaptera novaeangliae*) in the Benguela Upwelling System. *PLoS ONE,* 12, e0172002.

Fossette, S., Abrahms, B., Hazen, E.L., Bograd, S.J., Zilliacus, K.M., Calambokidis, J., Burrows, J.A., Goldbogen, J.A., Harvey, J.T., Marinovic, B., Tershy, B.R. & Croll, D.A. (2017) Resource partitioning facilitates coexistence in sympatric cetaceans in the California Current. *Ecology and evolution,* 7, 9085-9097.

Giraldeau, L.-A. & Caraco, T. (2000) Ch 8- Social Patch and Prey Models. *Social Foraging Theory*. Princeton University Press, Princeton, NJ, USA.

Goldbogen, J.A., Cade, D.E., Calambokidis, J., Friedlaender, A.S., Potvin, J., Segre, P.S. & Werth, A.J. (2017) How Baleen Whales Feed: The Biomechanics of Engulfment and Filtration. *Annual review of marine science,* 9, 1-20.

Goldbogen, J.A., Cade, D.E., Wisniewska, D.M., Potvin, J., Segre, P.S., Savoca, M.S., Hazen, E.L., Czapanskiy, M.F., Kahane-Rapport, S.R., DeRuiter, S.L., Gero, S., Tønnesen, P., Gough, W.T., Hanson, M.B., Holt, M., Jensen, F.H., Simon, M., Stimpert, A.K., Arranz, P., Johnston, D.W., Nowacek, D.P., Parks, S.E., Visser, F., Friedlaender, A.S., Tyack, P.L., Madsen, P.T. & Pyenson, N.D. (2019) Why whales are big but not bigger: Physiological drivers and ecological limits in the age of ocean giants. *Science,* 366, 1367-1372.

Goldbogen, J.A., Calambokidis, J., Croll, D.A., Harvey, J.T., Newton, K.M., Oleson, E.M., Schorr, G. & Shadwick, R.E. (2008) Foraging behavior of humpback whales: kinematic and respiratory patterns suggest a high cost for a lunge. *Journal of Experimental Biology,* 211, 3712-3719.

Goldbogen, J.A., Calambokidis, J., Croll, D.A., McKenna, M.F., Oleson, E., Potvin, J., Pyenson, N.D., Schorr, G., Shadwick, R.E. & Tershy, B.R. (2012) Scaling of lunge-feeding performance in rorqual whales: mass-specific energy expenditure increases with body size and progressively limits diving capacity. *Functional Ecology,* 26, 216-226.

Gordon, D.M. (2014) The ecology of collective behavior. *PLoS Biology,* 12, e1001805.

Guilpin, M., Lesage, V., McQuinn, I., Goldbogen, J.A., Potvin, J., Jeanniard-du-Dot, T., Doniol-Valcroze, T., Michaud, R., Moisan, M. & Winkler, G. (2019) Foraging energetics and prey density requirements of western North Atlantic blue whales in the Estuary and Gulf of St. Lawrence, Canada. *Marine Ecology Progress Series,* 625, 205-223.

Hazen, E.L., Friedlaender, A.S. & Goldbogen, J.A. (2015) Blue whale (*Balaenoptera musculus*) optimize foraging efficiency by balancing oxygen use and energy gain as a function of prey density. *Science Advances,* 1, e1500469.

Hazen, E.L., Friedlaender, A.S., Thompson, M.A., Ware, C.R., Weinrich, M.T., Halpin, P.N. & Wiley, D.N. (2009) Fine-scale prey aggregations and foraging ecology of humpback whales *Megaptera novaeangliae*. *Marine Ecology Progress Series,* 395, 75-89.

Hein, A.M., Altshuler, D.L., Cade, D.E., Liao, J.C., Martin, B.T. & Taylor, G.K. (2020) An Algorithmic Approach to Natural Behavior. *Current Biology,* 30, R663–R667.

Hein, A.M. & Martin, B.T. (2020) Information limitation and the dynamics of coupled ecological systems. *Nature Ecology & Evolution,* 4, 82-90.

Jaquet, N. (1996) Distribution and spatial organization of groups of sperm whales in relation to biological and environmental factors in the South Pacific.

Jarvis, T., Kelly, N., Kawaguchi, S., van Wijk, E. & Nicol, S. (2010) Acoustic characterisation of the broad-scale distribution and abundance of Antarctic krill (*Euphausia superba*) off East Antarctica (30-80 E) in January-March 2006. *Deep Sea Research Part II: Topical Studies in Oceanography,* 57, 916-933.

Jurasz, C.M. & Jurasz, V.P. (1979) Feeding modes of the humpback whale (*Megaptera Novaeangliae*) in southeast Alaska. *Scientific Reporting of Whales Research Institute,* 31, 69-83.

Kaartvedt, S., Røstad, A., Fiksen, Ø., Melle, W., Torgersen, T., Breien, M.T. & Klevjer, T.A. (2005) Piscivorous fish patrol krill swarms. *Marine Ecology Progress Series,* 299, 1-5.

Kahane-Rapport, S.R. & Goldbogen, J.A. (2018) Allometric scaling of morphology and engulfment capacity in rorqual whales. *Journal of Morphology*, 1-13.

Kirchner, T., Wiley, D.N., Hazen, E.L., Parks, S.E., Torres, L.G. & Friedlaender, A.S. (2018) Hierarchical foraging movement of humpback whales relative to the structure of their prey. *Marine Ecology Progress Series,* 607, 237-250.

LaScala-Gruenewald, D.E., Mehta, R.S., Liu, Y. & Denny, M.W. (2019) Sensory perception plays a larger role in foraging efficiency than heavy-tailed movement strategies. *Ecological Modelling,* 404, 69-82.

Leibniz, G. (1684) A new method for maxima and minima as well as tangents, which is neither impeded by fractional nor irrational quantitites, and a remarkable type of calculus for them (*translation*). *A Source Book in Mathematics, 1200–1800 (Struik, D. J.).* pp. 271-281. Harvard University Press.

Levin, S.A. (1992) The problem of pattern and scale in ecology: the Robert H. MacArthur award lecture. *Ecology,* 73, 1943-1967.

MacLennan, D.N., Fernandes, P.G. & Dalen, J. (2002) A consistent approach to definitions and symbols in fisheries acoustics. *ICES Journal of Marine Science,* 59, 365-369.

Magurran, A.E. & Henderson, P.A. (2003) Explaining the excess of rare species in natural species abundance distributions. *Nature,* 422, 714-716.

Mann, J. (2000) Unraveling the dynamics of social life. *Cetacean societies: field studies of dolphins and whales.* (eds J. Mann, R.C. Connor, P. Tyack & H. Whitehead), pp. 45-64. University of Chicago Press, , Chicago, Illinois, USA.

Mastick, N. (2016) The Effect of Group Size on Individual Roles and the Potential for Cooperation in Group Bubble-net Feeding Humpback Whales (*Megaptera novaeangliae*). M.S., Oregon State University.

Mayo, C.A. & Marx, M.K. (1990) Surface foraging behaviour of the North Atlantic right whale, Eubalaena glacialis, and associated zooplankton characteristics. *Canadian Journal of Zoology,* 68, 2214-2220.

Nickels, C.F., Sala, L.M. & Ohman, M.D. (2019) The euphausiid prey field for blue whales around a steep bathymetric feature in the southern California current system. *Limnology and Oceanography,* 64, 390-405.

Nicol, S., James, A. & Pitcher, G. (1987) A first record of daytime surface swarming by *Euphausia lucens* in the Southern Benguela region. *Marine Biology,* 94, 7-10.

Nowacek, D.P., Friedlaender, A.S., Halpin, P.N., Hazen, E.L., Johnston, D.W., Read, A.J., Espinasse, B., Zhou, M. & Zhu, Y. (2011) Super-aggregations of krill and humpback whales in Wilhelmina Bay, Antarctic Peninsula. *PLoS One,* 6, e19173.

Owen, K., Kavanagh, A.S., Warren, J.D., Noad, M.J., Donnelly, D., Goldizen, A.W. & Dunlop, R.A. (2017) Potential energy gain by whales outside of the Antarctic: prey preferences and consumption rates of migrating humpback whales (*Megaptera novaeangliae*). *Polar Biology,* 40, 277-289.

Pagel, M.D., Harvey, P.H. & Godfray, H. (1991) Species-abundance, biomass, and resource-use distributions. *The American Naturalist,* 138, 836-850.

Piatt, J.F. & Methven, D.A. (1992) Threshold foraging behavior of baleen whales. *Marine Ecology Progress Series,* 84, 205-210.

Pivorunas, A. (1979) The Feeding Mechanisms of Baleen Whales. *American Scientist,* 67, 432-440.

Preston, F.W. (1948) The commonness, and rarity, of species. *Ecology,* 29, 254-283.

Preston, F.W. (1962) The canonical distribution of commonness and rarity: Part I. *Ecology,* 43, 185-215.

Przybylski, A.K., Murayama, K., DeHaan, C.R. & Gladwell, V. (2013) Motivational, emotional, and behavioral correlates of fear of missing out. *Computers in Human Behavior,* 29, 1841-1848.

Rocha, R.C., Clapham, P.J. & Ivashchenko, Y.V. (2014) Emptying the oceans: a summary of industrial whaling catches in the 20th century. *Marine Fisheries Review,* 76, 37-48.

Santora, J.A., Zeno, R., Dorman, J.G. & Sydeman, W.J. (2018) Submarine canyons represent an essential habitat network for krill hotspots in a large marine ecosystem. *Scientific reports,* 8, 7579.

Slater, G.J., Goldbogen, J.A. & Pyenson, N.D. (2017) Independent evolution of baleen whale gigantism linked to Plio-Pleistocene ocean dynamics. *Proc. R. Soc. B,* 284, 20170546.

Southall, B.L., DeRuiter, S.L., Friedlaender, A., Stimpert, A.K., Goldbogen, J.A., Hazen, E., Casey, C., Fregosi, S., Cade, D.E. & Allen, A.N. (2019) Behavioral responses of individual blue whales (*Balaenoptera musculus*) to mid-frequency military sonar. *Journal of Experimental Biology,* 222, jeb190637.

Stephens, D.W. & Krebs, J.R. (1986) *Foraging theory*. Princeton University Press.

van der Hoop, J., Nousek-McGregor, A., Nowacek, D., Parks, S., Tyack, P. & Madsen, P. (2019) Foraging rates of ram-filtering North Atlantic right whales. *Functional Ecology,* 33, 1290-1306.

Watkins, J.L. & Murray, A.W.A. (1998) Layers of Antarctic krill, Euphausia superba: are they just long krill swarms? *Marine Biology,* 131, 237-247.

White, G.C. (1978) Estimation of plant biomass from quadrat data using the lognormal distribution. *Journal of Range Management*, 118-120.

Whitehead, H. (1983) Structure and stability of humpback whale groups off Newfoundland. *Canadian Journal of Zoology,* 61, 1391-1397.

Wiley, D.N., Ware, C., Bocconcelli, A., Cholewiak, D., Friedlaender, A., Thompson, M. & Weinrich, M. (2011) Underwater components of humpback whale bubble-net feeding behavior. *Behaviour,* 148, 575-602.

Wilson, R.P., Neate, A., Holton, M.D., Shepard, E.L., Scantlebury, D.M., Lambertucci, S.A., di Virgilio, A., Crooks, E., Mulvenna, C. & Marks, N. (2018) Luck in food finding affects individual performance and population trajectories. *Current Biology,* 28, 3871-3877. e3875.